Molecular Cell *21*, 319–330, February 3, 2006 ©2006 Elsevier Inc. DOI 10.1016/j.molcel.2005.12.011

Mapping Pathways and Phenotypes by Systematic Gene Overexpression

Richelle Sopko,[1,3] Dongqing Huang,[1,3] Nicolle Preston,[2,3] Gordon Chua,[2,3] Balázs Papp,[4] Kimberly Kafadar,[6] Mike Snyder,[5] Stephen G. Oliver,[4] Martha Cyert,[6] Timothy R. Hughes,[1,2,3] Charles Boone,[1,2,3,*] and Brenda Andrews[1,2,3,*]

[1] Department of Medical Genetics and Microbiology
University of Toronto
1 King's College Circle
Toronto, Ontario, M5S 1A8
Canada

[2] Banting and Best Department of Medical Research
University of Toronto
112 College Street
Toronto, Ontario, M5G 1L6
Canada

[3] The Terrence Donnelly Centre for Cellular and Biomolecular Research
University of Toronto
160 College Street
Toronto, Ontario M5S 3E1
Canada

[4] Faculty of Life Sciences
School of Biological Sciences
The University of Manchester
The Michael Smith Building
Oxford Road, Manchester M13 9PT
United Kingdom

[5] Department of Molecular, Cellular and Developmental Biology
Yale University
New Haven, Connecticut 06620

[6] Department of Biological Sciences
147 Lokey Laboratory
337 Campus Drive
Stanford University
Stanford, California 94305

Summary

Many disease states result from gene overexpression, often in a specific genetic context. To explore gene overexpression phenotypes systematically, we assembled an array of 5280 yeast strains, each containing an inducible copy of an *S. cerevisiae* gene, covering >80% of the genome. Approximately 15% of the overexpressed genes (769) reduced growth rate. This gene set was enriched for cell cycle-regulated genes, signaling molecules, and transcription factors. Overexpression of most toxic genes resulted in phenotypes different from known deletion mutant phenotypes, suggesting that overexpression phenotypes usually reflect a specific regulatory imbalance rather than disruption of protein complex stoichiometry. Global overexpression effects were also assayed in the context of a cyclin-dependent kinase mutant (*pho85*Δ). The resultant gene set was enriched for Pho85p targets and identified the yeast calcineurin-responsive transcription factor Crz1p as a substrate. Large-scale application of this approach should provide a strategy for identifying target molecules regulated by specific signaling pathways.

*Correspondence: charlie.boone@utoronto.ca (C.B.); brenda.andrews@utoronto.ca (B.A.)

Introduction

Observing the effects of gene perturbation on cells or organisms has long been a standard strategy in biological research (Forsburg, 2001). The genetic accessibility of the budding yeast *S. cerevisiae* has allowed the development of genome-wide loss-of-function mutant collections, including gene deletion (Giaever et al., 2002) and titratable promoter alleles (Mnaimneh et al., 2004), for systematic scrutiny of gene function. The development of high-throughput methods for combining different gene deletion or loss-of-function alleles within a single cell has enabled systematic evaluation of synthetic or synergistic genetic interactions (Pan et al., 2004; Tong et al., 2004). The resultant complex genetic networks define gene function and map functional relationships amongst genes and pathways (Kelley and Ideker, 2005; Tong et al., 2004; Zhang et al., 2005). Nevertheless, 30% of yeast genes remain functionally uncharacterized, and the roles of many previously characterized genes remain obscure ([Hughes et al., 2004]; *Saccharomyces* Genome Database, http://www.yeastgenome.org/cache/genomeSnapshot.html). For example, the wiring diagrams of signaling pathways are largely incomplete; there are hundreds of kinases and phosphatases in yeast (Manning et al., 2002) and very little is known about their targets, highlighting the need for new systematic genetic approaches. The analysis of gene overexpression phenotypes provides a unique insight into gene function, because it can lead to hyper or neomorphic effects, often due to misregulation (Akada et al., 1997; Boyer et al., 2004; Espinet et al., 1995; Herskowitz, 1987; Liu et al., 1992; Stevenson et al., 2001; Zhang et al., 1999). The importance of understanding the mechanisms of biological perturbation caused by gene overexpression is underscored by the prevalence of gene hyperactivation or amplification in many human disease states. In a more general sense, the need to restrain increased gene dosage is predicted to provide a significant constraint in the evolution of gene expression (Wagner, 2005).

Often, the effects of gene dosage may only be apparent in a specific genetic context, either reversing (dosage suppression) or exacerbating (dosage enhancement) a mutant phenotype. Synthetic dosage lethality (SDL) is based on the idea that increasing levels of a protein may have no effect on the growth of an otherwise wild-type (wt) strain but may cause a clear phenotype—such as lethality—in a mutant strain with reduced activity of an interacting protein (Kroll et al., 1996; Measday and Hieter, 2002). SDL defined a broad spectrum of interacting genes encoding components of the yeast kinetochore and the origin recognition complex (Kroll et al., 1996; Measday et al., 2002, 2005). Information derived

from an SDL interaction can be functionally rich; for example, a strain with reduced activity of the anaphase promoting complex (APC) cannot tolerate high levels of *CLB2*, which encodes an APC substrate, suggesting that SDL will be an effective tool for identification of novel enzyme targets (Irniger et al., 1995). Systematic SDL screens may provide a general genetic strategy for linking signaling molecules to their target proteins.

We describe here the construction of an ordered array of yeast strains each overexpressing a unique gene, covering 85% of all yeast genes. We demonstrate the use of the genome-wide gene overexpression library as a new tool for functional genomics analysis in yeast. Whereas previous large-scale genetic studies have focused on assays of deletion mutant arrays, the overexpression array enables comprehensive examination of gain-of-function phenotypes. We present a systematic analysis of gene overexpression phenotypes in yeast and find that ~15% of genes reduced growth rate when overexpressed, often due to pathway activation, allowing us to ascribe function to uncharacterized genes and to gain insight into the mechanisms leading to gene overexpression phenotypes. We combined our overexpression array with synthetic genetic array (SGA) analysis, enabling automated SDL screens for rapid assessment of overexpression phenotypes in any mutant background. As a proof of concept, we show that comprehensive overproduction of genes in cells lacking the Pho85 cyclin-dependent kinase (Cdk) identified several known targets, as well as an additional substrate. This screen validates the method of systematic synthetic dosage lethality by using the plasmid-based overexpression array to identify kinase targets.

Results

Systematic Examination of Gene Overexpression Causing Slow Growth Identifies 769 Genes with a Bias toward Specific Biological Functions

To examine gene overexpression effects on a global scale, we constructed an ordered array of 5280 yeast strains, each conditionally overexpressing a unique yeast gene, covering 85% of all yeast genes. Each strain carries a different yeast ORF tagged at its amino terminus with GST and expressed from the inducible *GAL1/10* promoter on a multicopy plasmid (Zhu et al., 2001). To catalog the spectrum of genes that affect cellular fitness when overexpressed, the array was transferred to medium containing galactose, and each strain was examined for defects in colony formation. A total of 769 strains, representing ~15% of all yeast genes, showed a galactose-specific slow-growth phenotype (Figure 1A and Table S6 available in the Supplemental Data with this article online). The resultant toxic gene set overlapped significantly with other studies that searched for overexpression phenotypes in nonarrayed cDNA or genomic libraries (Akada et al., 1997; Boyer et al., 2004; Espinet et al., 1995; Liu et al., 1992; Stevenson et al., 2001), suggesting that most of the observed phenotypes occur independently of the GST fusion (see Discussion). Surprisingly, there was no bias within the dataset for essential genes (146/769 genes are essential [18.9%] versus 1050/5800 [18.1%] for the genome as a whole). On the other hand, the 769 genes were highly biased for genes with particular GO biological process or molecular function annotations, including genes involved in transport, cytoskeletal organization, transcriptional regulation, the cell cycle, and secretion (Figure 1B and Table S5). In addition, the toxic gene set was enriched for genes annotated with specific activities, including transcription factors and signaling proteins such as phosphatases, kinases, and transporters, suggesting that cells are more sensitive to perturbation of pathways defined by these regulators (Figure 1B and Table S5).

Systematic Phenotypic Analysis of the Toxic Gene Set

To infer mechanisms of toxicity caused by gene overexpression, we systematically analyzed the morphology of each of the 769 toxic strains by microscopy, examining 27 morphological descriptors, including cell and nuclear morphology, bud scar pattern, and the distribution of filamentous actin (Figure 2A). A subset of 184 of the 769 strains examined displayed a mutant morphological phenotype after 5 hr of gene induction (Figures 1A, Table S7, and http://142.150.56.93:8080/htmis/htmisquery.jsp). Of these, 120 (~65%) exhibited a cell cycle arrest or delay as determined by fluorescence-activated cell sorting (FACS) (Figure 1A and Table S8). Given this large representation of cell cycle phenotypes, we asked if the corresponding genes tended to show a cell cycle-regulated pattern of gene expression in normal cells. Genes expressed periodically during the cell cycle (de Lichtenberg et al., 2005) were more likely to show an overexpression phenotype ($p = 0.017$), and in particular, this tended to cause abnormal morphology [$p < 10^{-13}$] or cell cycle arrest [$p < 10^{-14}$] (Table S3). When the analysis is limited to genes known to function in the mitotic cell cycle, we still find that overexpression of periodically expressed genes is more likely to cause cell cycle arrest ($p = 0.008$) or abnormal morphology ($p = 0.006$) than constitutively expressed cell cycle genes (Table S3), indicating that unscheduled expression of genes that are usually expressed periodically often leads to toxicity.

There Exists No Bias within the Toxic Gene Set for Proteins within Macromolecular Complexes

The "balance hypothesis" posits that deviations from the normal stoichiometry of members of protein complexes cause haploinsufficiency and predicts a concordance between haploinsufficient and overexpression phenotypes (Papp et al., 2003). However, when we examined protein complex compositions assembled from an annotated list of protein complexes deposited in the MIPS Comprehensive Yeast Genome Database (Mewes et al., 2004) and three large-scale protein complex purification studies (Gavin et al., 2002; Ho et al., 2002; Krogan et al., 2004), we found no significant enrichment for the toxic gene set ($p = 0.18$), the abnormal morphology subset ($p = 0.97$), or the cell cycle arrest subset ($p = 0.73$; Table S3). We also found little correlation between our dataset and a set of genes showing significant haploinsufficiency under nutrient-rich growth conditions (Deutschbauer et al., 2005) ($p = 0.2$ for toxic dataset, $p = 0.21$ for morphology subset, and $p = 0.34$ for cell cycle subset). Thus, these findings do not support the balance hypothesis as a primary mechanism

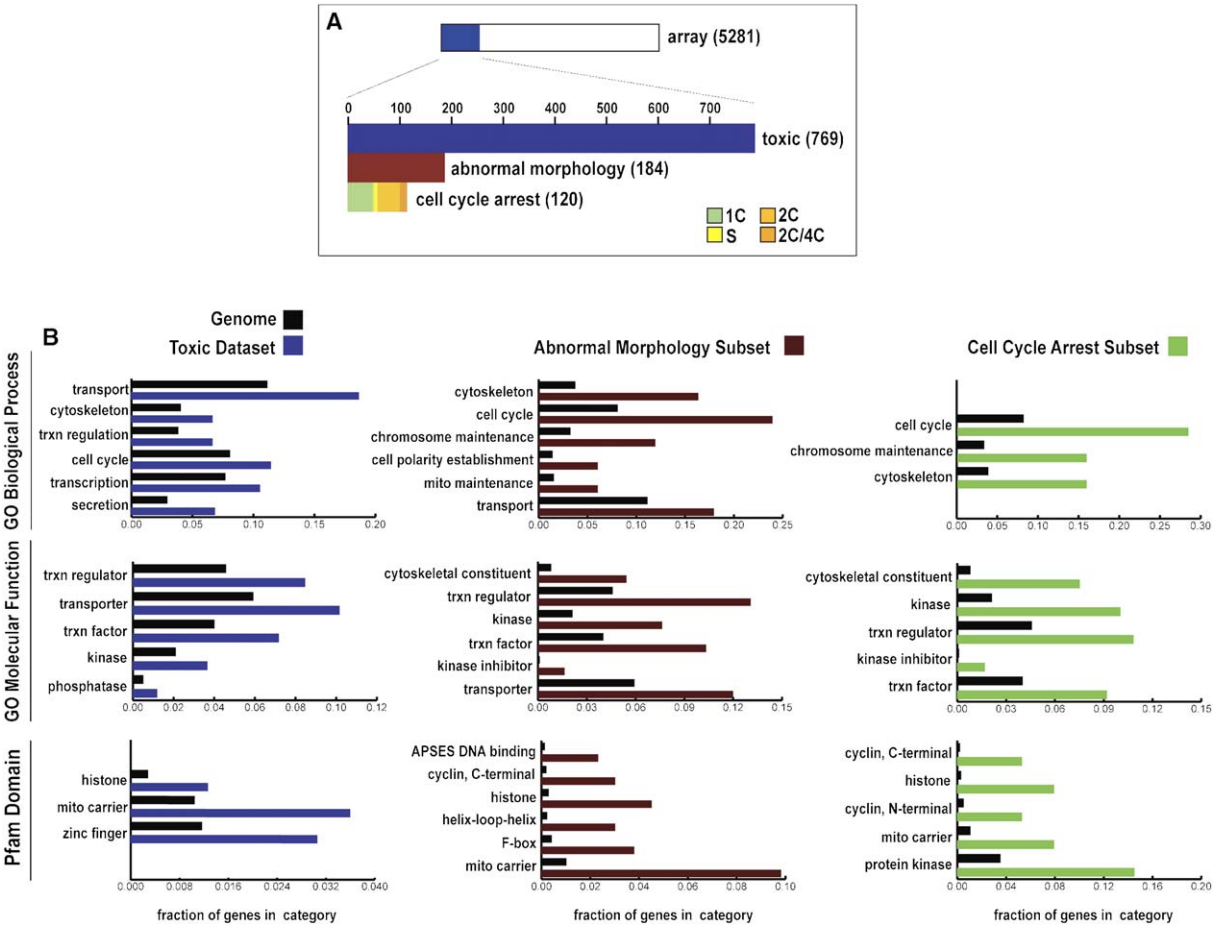

Figure 1. Features of the *S. cerevisiae* Toxic Gene Set

(A) Schematic representation of the *S. cerevisiae* overexpression array. The top bar represents the 5280 genes present in the array. The blue bar represents the 769 genes that caused slow growth upon overexpression; the red bar represents the subset of toxic genes (184) that caused an aberrant morphological phenotype. The subset of toxic genes that produced a measurable cell cycle phenotype upon overexpression (120) is depicted by the multicolored bar: shift toward 1C DNA content, green; accumulation in S phase, yellow; shift toward 2C DNA content, light orange; and shift toward 4C DNA content, dark orange.

(B) Enrichment within the toxic gene datasets for biological processes and molecular functions. Genes in the toxic dataset (blue columns), abnormal morphology subset (brown columns), or cell cycle arrest subset (green columns) were classified by gene ontology (GO) biological process and molecular function terms and the Pfam protein domain database by FunSpec (http://funspec.med.utoronto.ca/). Enrichment in the various categories relative to the entire yeast genome (black columns) is depicted (see Supplemental Data for details of the analysis).

for overexpression lethality. Rather, they are consistent with the primary mechanism of haploinsufficiency reflecting insufficient protein production (Deutschbauer et al., 2005).

Most Overexpression Phenotypes Do Not Resemble Deletion Mutant Phenotypes

To classify the overexpression phenotypes as gain- or loss-of-function, we compared them to deletion phenotype information derived from large-scale characterizations (Giaever et al., 2002; Jorgensen et al., 2002; Mnaimneh et al., 2004; Saito et al., 2004) and the literature (Table S9). In total, the overexpression of 42 genes caused a phenotype resembling that associated with the gene deletion (Figure 2B). For example, overexpression of *SHS1* or *CDC11*, both components of the septin ring complex, causes cells to become large and elongated with extremely hyperpolarized buds. This phenotype is similar to that observed for mutants of many septin-encoded genes (Kim et al., 1991) and is consistent with data from other experiments indicating that these proteins participate in a complex where protein stoichiometry is critical. Indeed, for the 42 cases in which a gene overexpression phenotype caused a loss-of-function phenotype, 25 are known to participate in multiprotein complexes (Table S9). In this subset of cases, the mechanism of overexpression lethality is most probably consistent with the balance hypothesis. However, the other 142 genes in the morphological subset produced phenotypes that did not resemble those of null mutants (in the case of nonessential genes) or of tetracycline-repressible promoter strains (in the case of essential genes). Thus, the majority of the overexpressed genes exhibit a hyperactive gain of function phenotype or a novel unregulated effect. There are some clear examples of hyperactive phenotypes; for instance, overexpression of *FAR1*, which encodes an inhibitor of the cell cycle kinase Cdc28p, leads to a G1 arrest phenotype, as

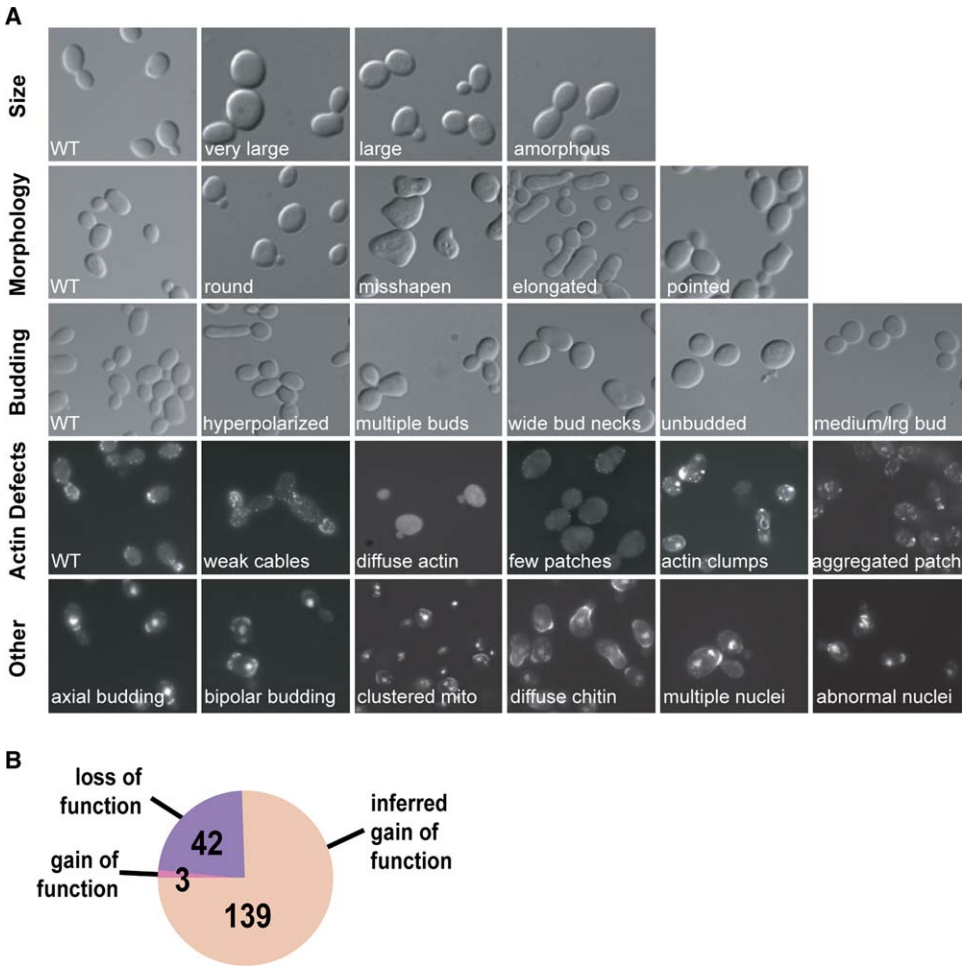

Figure 2. Characteristics of the *S. cerevisiae* Toxic Gene Set Based on Morphology

(A) The morphology of each of the 769 strains demonstrating slow growth upon gene overexpression was examined after a 5 hr exposure to galactose. Nuclei, actin, and bud scars of formaldehyde-fixed cells were visualized with DAPI, rhodamine-conjugated phalloidin, and Fluorescence Brightener, respectively. Morphology of cells was scored based on one or more of 27 morphological descriptors. The strains shown are very large, p*GAL-UPC2*; large, p*GAL-BIK1*; amorphous, p*GAL-SPT23*; round, p*GAL-MET4*; misshapen, p*GAL-STE4*; elongated, p*GAL-GIC2*; pointed, p*GAL-HML*α*2*; hyperpolarized, p*GAL-SHS1*; multiple buds, p*GAL-IQG1*; wide bud necks, p*GAL-YDL129W*; unbudded, p*GAL-XBP1*; medium/large budded, p*GAL-SHE1*; weak cables, p*GAL-KIN3*; diffuse actin, p*GAL-SNC1*; few patches, p*GAL-YDL129W*; actin clumps, p*GAL-ENT2*; aggregated patches, p*GAL-YPR171W*; bipolar budding, p*GAL-MAT*α*2*; clustered mitochondria, p*GAL-SCO2*; diffuse chitin, p*GAL-SOK2*; multiple nuclei, p*GAL-BIK1*; and abnormal nuclei, p*GAL-NUP1.*

(B) Classification of overexpression phenotypes. Overexpression phenotypes for the 184 genes that caused a significant morphological defect as assessed by a number of descriptors (Figure 2A) were compared to deletion phenotypes reported in the literature and large-scale studies (Table S4). The number of genes whose overexpression caused a loss-of-function, clear gain-of-function, or inferred gain-of-function phenotype is depicted.

does *STE4*, which controls G1 arrest in response to pheromone signaling (Henchoz et al., 1997; Whiteway et al., 1990). The preponderance of signaling molecules and transcription factors in our "abnormal morphology" and "cell cycle" subsets suggests that many of these signaling molecules may be deregulated upon overexpression. Indeed, a microarray analysis of 50 different transcription factors has allowed us to define regulatory networks and link transcription factors to their binding sites (G.C. and T.H., unpublished data).

Assessment of an Overexpression Phenotype Allows Annotation of Genes Lacking a Loss-of-Function Phenotype

To further substantiate the view that gain of function accounts for overexpression phenotypes, we considered the case of *WHI4*. No function for *WHI4* has been uncovered solely from deletion mutant analysis; a deletion mutant of *WHI4* has no phenotype. *WHI4*, however, is considered to be partially redundant with *WHI3* (Nash et al., 2001). Both possess an RNA recognition motif (RRM), which in the case of Whi3p has been shown to regulate the mRNA of *CLN3*, a G1 cyclin (Gari et al., 2001). In addition to RNA binding, Whi3p localizes the Cdc28p-Cln3p Cdk complex to the cytoplasm by directly binding Cdc28p (Wang et al., 2004). We found that overexpression of *WHI4* caused a G1 arrest, as defined by an accumulation of large, unbudded cells (Figure 3A) with 1C DNA content (Figure 3B). Overexpression of *WHI3* caused a similar phenotype (data not shown). To substantiate a G1 role for *WHI4*, we conducted microarray experiments to assess global changes in the regulation

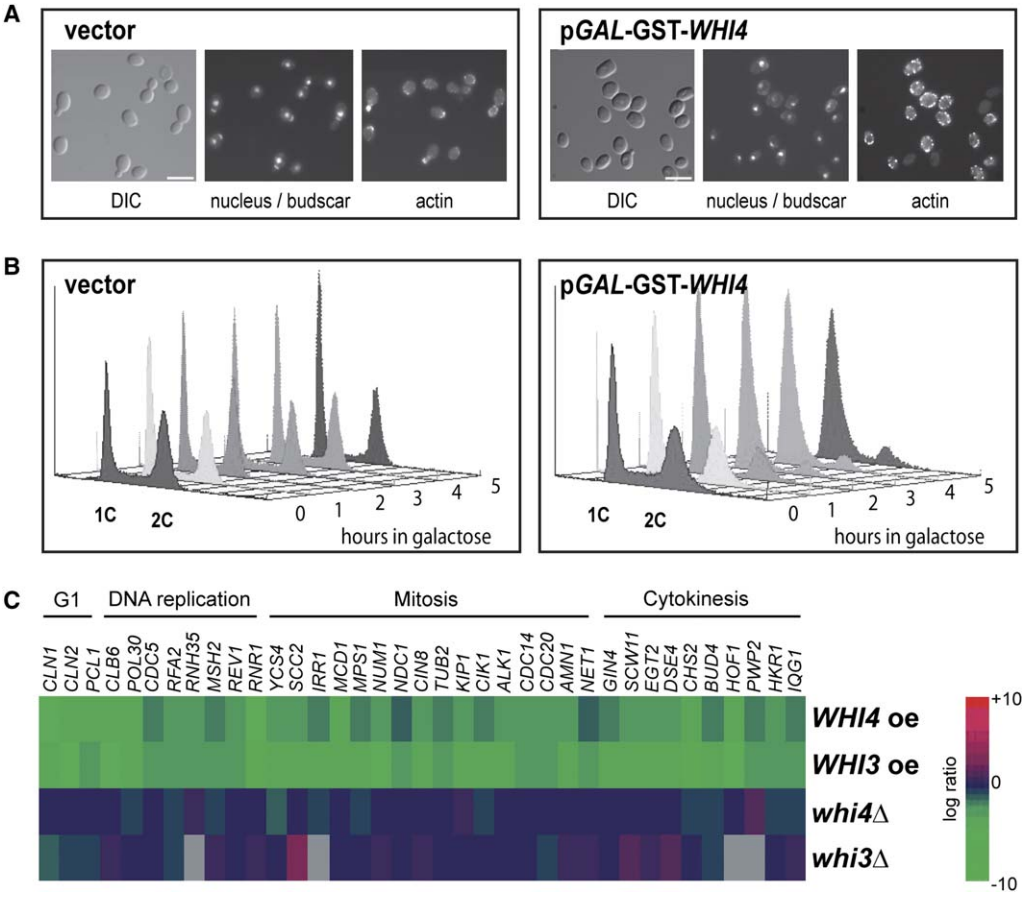

Figure 3. Gene Overexpression Defines a G1 Role for *WHI4*

(A and B) Overexpression of *WHI4* causes a G1 phase arrest. (A) Wt strains carrying either vector (left) or p*GAL*-GST-*WHI4* (right) were induced in galactose for 5 hr and examined by DIC microscopy (DIC panel) or fixed and stained with DAPI, rhodamine-conjugated phalloidin, and Fluorescence Brightener. Cells were visualized at 100× magnification with fluorescence microscopy using excitation and emission wavelengths appropriate for DAPI and Fluorescence Brightener to visualize the nucleus and bud scars, respectively (middle panels), or rhodamine to visualize filamentous actin (right panels). Size bar is 10 μm. (B) FACS analysis of DNA content in cells overexpressing *WHI4*. FACS analysis was performed on strains carrying either empty vector (left) or the *GAL*-GST-*WHI4* plasmid (right). Samples were taken at 0, 1, 2, 3, 4, and 5 hr after galactose shift, and Sytox Green-stained cells were analyzed by FACS. The positions of cells with unreplicated (1C) and replicated (2C) DNA are indicated. (C) Overexpression of *WHI4* represses mitotic cell cycle genes. Genome-wide expression profiles were determined for strains overexpressing *WHI4* (*WHI4* oe), *WHI3* (*WHI3* oe) after 3 hr of galactose induction, or for strains deleted for *WHI4* or *WHI3* (*whi4*Δ, *whi3*Δ). The cluster was generated by MatLab software; genes with annotated cell cycle functions are shown. The color ratio scale is to the right. Scale indicates fold change.

of gene transcription (Figure 3C). These experiments revealed that the overexpression of *WHI4* resulted in the specific downregulation of genes involved in mitotic cell cycle regulation ($p = 2.3\ E^{-4}$), including those encoding the G1 and S phase cyclins. This transcriptional response was also seen when either a C-terminally FLAG-tagged version of *WHI4* (data not shown) or *WHI3* was overexpressed (Figure 3C). Thus, the *WHI4* overexpression phenotype appears to reflect a G1 role analogous to that of *WHI3*, an inference that can be derived solely from analysis of *WHI4* overexpression.

Array-Based SDL

Most genes do not cause a dramatic fitness defect when overexpressed in wt cells. However, overexpression phenotypes may be revealed within the context of regulatory mutants that enhance gain-of-function phenotypes, a phenomenon known as SDL (see Introduction) (Kroll et al., 1996; Measday and Hieter, 2002). With this in mind, we used SGA analysis (Tong et al., 2001, 2004) to cross a deletion mutant allele of *PHO85* into the overexpression array. Pho85p is a multifunctional Cdk known to associate with ten different cyclin regulatory subunits to discharge numerous biological functions, including cell cycle control, cell polarity establishment, and phosphate and glycogen metabolism (Moffat et al., 2000), but its full substrate repertoire remains unknown. All known Pho85p substrates are negatively regulated by phosphorylation; hence, we reasoned that overexpression of an unfettered substrate might be detrimental to the cell and lead to an SDL phenotype (Figure 4A). The *pho85Δ* SDL screen (Figure 4B) uncovered 65 interactions (Figure 5A and Table S4), four of which were with known Pho85p substrates (Pho4p, Gsy1p, Gsy2p, and Gcn4p), a result highly unlikely to occur by chance ($p = 7.1\ E^{-7}$). This list included genes involved in budding and polarity establishment, vacuolar function, transcription, metabolism, cell cycle regulation,

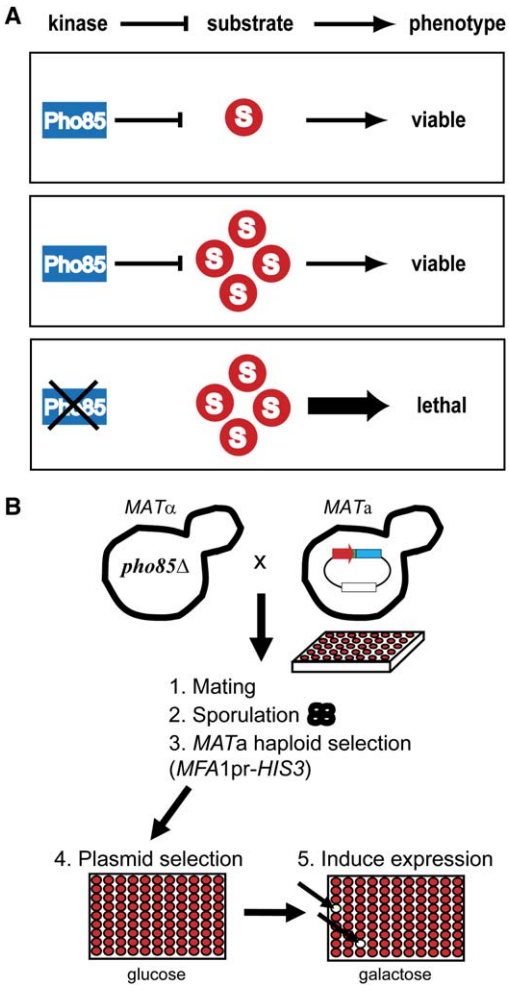

Figure 4. Array-Based SDL Screens to Identify Kinase Substrates

(A) Schematic illustrating the conceptual basis for SDL screening to identify kinase targets.

(B) Schematic illustration of systematic SDL screening. A *MAT*α strain carrying a query mutation (*pho85*Δ) and the *MFA1-HIS3* reporter is crossed to the ordered array of yeast overexpression mutants (*MAT*a), each carrying a p*GAL1/10*-GST-6×His-*ORF* plasmid. Diploids are selected and sporulated, and *MAT*a haploids carrying the query mutation (*pho85*Δ) and an overexpression plasmid are isolated by selection for the mating type-specific reporter (*MFA1-HIS3)* as well as query mutation and plasmid markers. Haploids are pinned to galactose to induce expression from the plasmid-based *GAL1-10* promoter. Colony sizes on galactose are compared to those on glucose to identify those strains with a galactose-specific growth defect reflecting sensitivity to overexpression of the plasmid-borne gene. Results are compared to the effects of gene overexpression in a wt strain to identify SDL phenotypes specific to deletion of the query gene.

and cell wall organization, consistent with previous work implicating Pho85p in cell morphogenesis and vacuole function (Huang et al., 2002; Moffat and Andrews, 2004).

Crz1p Is a Target of the Pho85p-Pho80p Cdk

To prioritize our list of 65 potential kinase substrates for direct kinase targets to further investigate, we compared the results of our SDL screen with the results of a protein chip experiment that cataloged in vitro substrates for several different cyclin forms of Pho85p (Ptacek et al., 2005). Crz1p was among the proteins hit strongly in the Pho85p protein microarray assay that was also identified in our *pho85⊿* SDL screen (Figure 5A). Crz1p is the yeast analog of mammalian NFATc transcription factors; both are activated by the calcium-dependent phosphatase calcineurin to drive programs of gene expression (Cyert, 2003). Crz1p acts through upstream calcineurin-dependent response elements (CDREs) to activate genes that promote cell survival during stress (Stathopoulos and Cyert, 1997). Calcineurin desphosphorylates Crz1p and causes its rapid translocation from the cytosol to the nucleus. Both the casein kinase I isoform Hrr25p and cyclic AMP-dependent protein kinase A (PKA) act to negatively regulate Crz1p, but phenotypic assessment suggests that other potent Crz1p kinases must exist (Kafadar and Cyert, 2004; Kafadar et al., 2003).

If Pho85 were phosphorylating Crz1p in vivo, a specific Pho85-cyclin complex may be involved. Like the *pho85*Δ kinase mutant, we predicted *CRZ1* overexpression in a mutant lacking the relevant Pho85 cyclin(s) would result in slow growth. Only a *pho80*Δ cyclin mutant was sensitive to *CRZ1* overexpression (Figure 6A), likely reflecting specificity of Pho85p-Pho80p for Crz1p. Other evidence implicated Pho85p-Pho80p as the relevant in vivo kinase complex: (1) the activity of a *CDRE-lacZ* reporter was reproducibly elevated in *pho85*Δ or *pho80*Δ mutant strains in the absence or presence of calcium, consistent with a role for Pho85p in regulating Crz1p activity (Figure 6B); (2) when *PHO80* was overexpressed, the increase in calcium-dependent CDRE-*lacZ* activity normally seen in a wt strain was dramatically decreased (Figure 6B); and (3) Pho80p-Pho85p affected GFP-Crz1p localization (Figure 6C). After adaptation to calcium stress, Crz1p relocalizes from the nucleus to the cytoplasm. The phosphorylation status of Crz1p has been shown to influence this shuttling by altering its rates of nuclear import and export (Boustany and Cyert, 2002; Polizotto and Cyert, 2001; Stathopoulos-Gerontides et al., 1999). To determine whether Pho85p-Pho80p influenced the dynamics of Crz1p shuttling, we performed time-lapse microscopy on cells coexpressing GFP-*CRZ1* and *PHO80*. After a 2 min exposure of wt cells to 100 mM $CaCl_2$, ~33% of cells had detectable nuclear GFP-Crz1p signal. This increased to ~76% of cells after 15 min (Figure 6C). By contrast, only ~8% of cells overexpressing *PHO80* had detectable nuclear GFP-Crz1p signal immediately after exposure to 100 mM calcium (Figure 6C, t = 2 min). Moreover, the *PHO80*-expressing cells showed a more rapid loss of nuclear GFP signal than wt cells exposed to the same concentration of calcium for 25 min (Figure 6C). Immunoblotting for GFP-Crz1p reveals that this decrease in nuclear signal is not due to any decreased stability of the protein in the *PHO80* overexpressing strain relative to wt (Figure S1). These observations suggest that higher Pho80p-Pho85p kinase activity results in increased GFP-Crz1p nuclear export and/or decreased GFP-Crz1p nuclear import and is in agreement with previous studies demonstrating the effects of phosphorylation on Crz1p localization (Boustany and Cyert, 2002; Polizotto and Cyert, 2001; Stathopoulos-Gerontides et al., 1999).

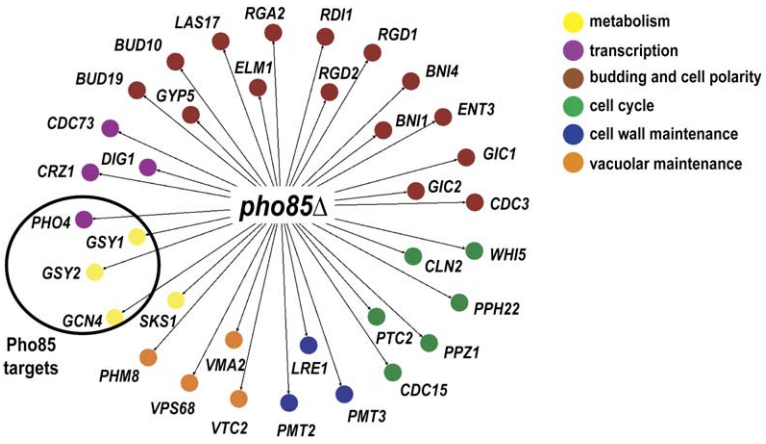

Figure 5. Genetic Interactions Identified from SDL Screening with *pho85*Δ

Network diagram summarizing SDL interactions between *pho85* deletion and strains in the overexpression array. Genes are represented as nodes, and interactions are represented as edges. The nodes are colored according to their GO biological process, and some were manually annotated from the literature. A complete list of *pho85*Δ SDL interactions is compiled in Table S5. Known Pho85p substrates are highlighted by a circle.

Crz1p possesses nine potential Pho85 phosphorylation sites (S/TP). Using purified Crz1p protein fragments, we performed in vitro kinase assays with recombinant Pho85-Pho80p to identify relevant sites of phosphorylation (Figure 6D). Both full-length Crz1p and a region of Crz1p (amino acids 181–340) possessing five potential sites were excellent in vitro substrates for Pho80p-Pho85p. Two of these sites (T202 and S213) lie within the serine-rich region (SRR; considered to be required for calcineurin's regulation of Crz1p) and within a region required for nuclear export. The three other sites (T319, S321, and T330) lie adjacent to or within the PIISIQ motif where calcineurin is known to dock. Mutations T202A and S213A mimicked the deletion of *PHO80* in a CDRE-*lacZ* reporter assay (Figure 6E, Crz1TSA). Activity of the Crz1p-specific CDRE-*lacZ* reporter was increased in the double mutant, and this was exacerbated by mutation of those sites predicted to be phosphorylated by Hrr25p (S231A and S234A) (Figure 6E, quadruple). These results reveal additive roles for Pho80-Pho85p and Hrr25p in Crz1p regulation. Thus, our systematic SDL screen revealed a physiological role for the Pho80p-Pho85p kinase and established a previously unappreciated link between a Cdk and calcium signaling.

Discussion

Previous large-scale studies with budding yeast have focused on applications of the deletion mutant collection (Giaever et al., 2002; Winzeler et al., 1999), which has arguably revolutionized the functional characterization of yeast genes (Scherens and Goffeau, 2004). Although extremely powerful, deletion mutant experiments are generally restricted to the characterization of loss-of-function phenotypes, an approach that is pragmatically limited by the lack of easily assayable or informative phenotype for loss-of-function mutations in an estimated two-thirds of genes in yeast, flies, and *C. elegans* (Rorth et al., 1998). In this study, we explore the potential for high-throughput genetic analysis (Tong et al., 2001) with a genome-wide "overexpression array," in which each strain on the array overexpresses a unique yeast gene. The overexpression array enables systematic assay of gain-of-function phenotypes, including defects associated with misregulation of essential genes.

We performed a systematic analysis of gene overexpression in yeast and identified a set of 769 toxic genes that compromise cellular fitness when overexpressed. Our dataset of toxic genes (~15% of the genome) overlaps significantly with datasets produced from other random screens performed by using cDNA libraries or genomic DNA libraries (see Supplemental Data for details; [Espinet et al., 1995; Akada et al., 1997; Stevenson et al., 2001; Boyer et al., 2004]). Because our study of overexpression phenotypes is systematic, and because we can integrate our dataset with other large yeast functional genomics information, including the set of haploinsufficient genes, cell cycle-regulated genes, and essential genes, we can address general mechanistic questions about overexpression phenotypes. One central, and still unanswered, question in genetics is what determines genetic dominance in diploid organisms. A loss-of-function mutation in one allele of a diploid pair is recessive for most genes, but we nevertheless know that certain genes show haploinsufficient phenotypes (i.e., inactivity of one allele reduces fitness). Although the mechanism of haploinsufficiency is unknown, it has been suggested that such genes are sensitive to decreased dosage because the heterozygote produces less protein than is required to sustain a normal phenotype (the insufficiency hypothesis, see Deutschbauer et al. [2005]). An alternate view, the balance hypothesis, posits that it is not the absolute level of a protein that is important but, rather, the relative dosage of physically interacting proteins (i.e., those participating in stoichiometric complexes). Thus, a decrease in the amount of a protein could be harmful because it causes an imbalance in the concentrations of interacting subunits (Papp et al., 2003; Veitia, 2002, 2005). The fact that genes encoding proteins that are subunits of complexes are more likely to be haploinsufficient than other genes (Papp et al., 2003) is compatible with both hypotheses. Therefore, the only way to discriminate between the two theories is to analyze overexpression phenotypes. According to the balance hypothesis, genes encoding subunits of complexes should more frequently be toxic when overexpressed. However, the lack of large-scale overexpression data meant that it was impossible to resolve this issue in a definitive manner. Here, we attack this question in a comprehensive manner by analyzing genome-wide data generated by our overexpression

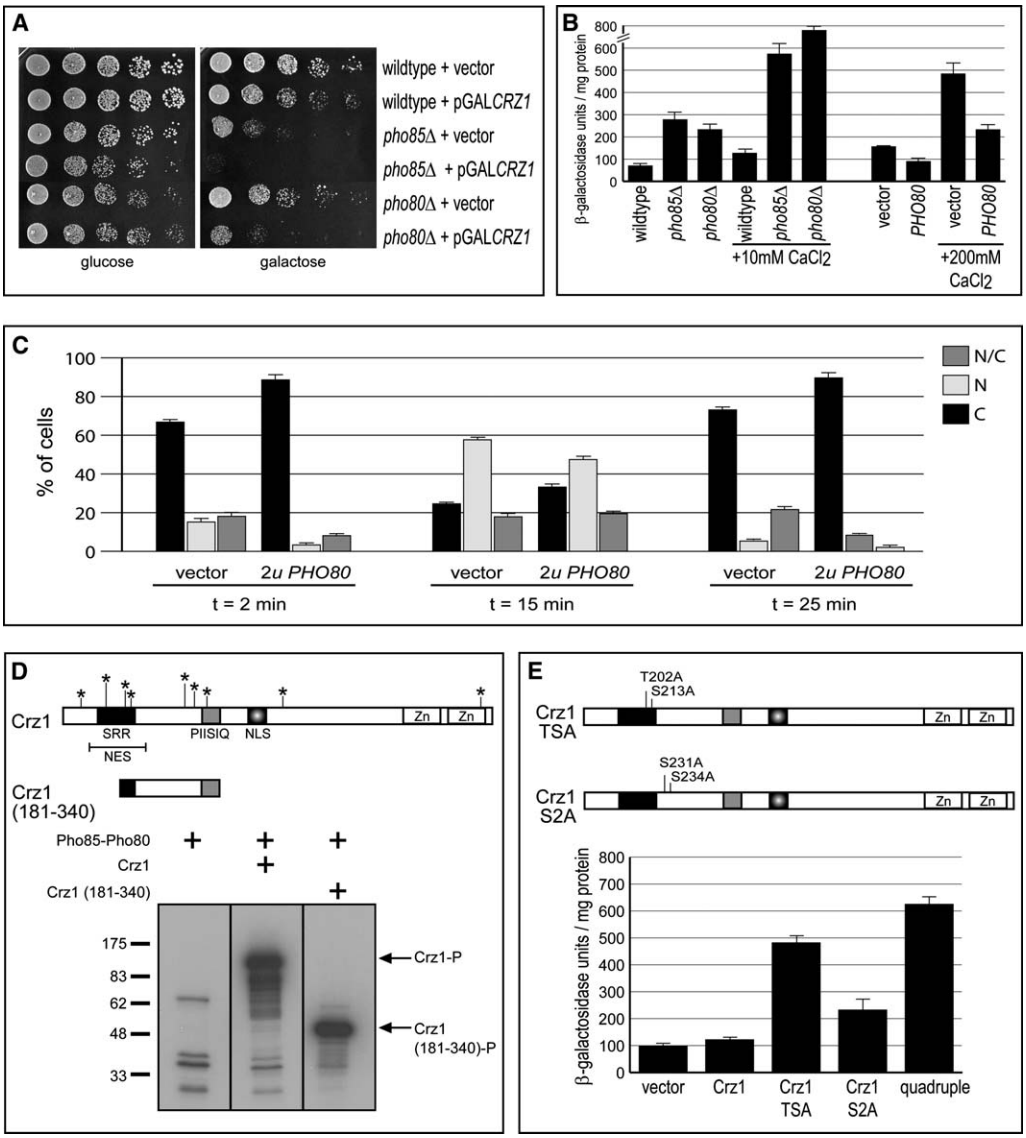

Figure 6. Crz1p Is a Bona Fide Substrate of the Pho80p-Pho85p Kinase

(A) Overexpression of *CRZ1* causes a severe growth defect in the absence of *PHO85* or the *PHO80* cyclin. Isogenic wt (BY263), *pho85*Δ (BY391), and *pho80*Δ (BY490) strains bearing either p*GAL1/10*-GST-6×His-*CRZ1* or vector (pEGH) were spotted in serial 15-fold dilutions on either glucose (left) or galactose (right) medium and incubated at 30ºC.

(B) Pho80p-Pho85p affects Crz1p transcriptional activity. The four bars on the right illustrate the activity of Crz1p in response to overexpression of *PHO80*. Cells carrying an integrated 4×CDRE::*lacZ* reporter (ASY832) and either vector or pGPD*PHO80* (pBA1810) were cultured, and β-galactosidase activity was measured. Where indicated, 200 mM $CaCl_2$ was added for 3 hr. The six bars on the left show activity of Crz1p in response to deletion of *PHO85* or *PHO80*. Where indicated, 10 mM $CaCl_2$ was added for 3 hr. Data are the mean (±SEM) of three independent isolates.

(C) Localization of GFP-Crz1p in response to overexpression of *PHO80*. Wt cells (BY263) expressing 3×GFP-Crz1 (pLMB127) and either vector (p425GPD) or pGPD-*PHO80* (pBA1810) were induced for 5 hr in the absence of methionine. Then, 100 mM $CaCl_2$ (t = 0) was added, and cells were examined at the indicated time points. Between 150 and 300 cells were counted for each time point. Black bars represent cells with exclusively cytoplasmic (C) GFP-Crz1p; light gray bars represent cells with exclusively nuclear (N) GFP-Crz1p; and dark gray bars represent cells with an intermediate nuclear/cytosolic localization (N/C) of GFP-Crz1p. Standard deviation is represented by error bars (see Supplemental Data for details).

(D) Pho80p-Pho85p phosphorylates Crz1p in vitro. Recombinant GST-Crz1p and a purified Crz1p fragment (amino acids 181–340) were incubated with recombinant Pho85p-Pho80p kinase purified from insect cells and γ^{32}P-ATP. The schematic of full-length Crz1p and the smaller fragment shows locations of relevant Crz1p protein domains (abbreviations: NES, nuclear export signal; NLS, nuclear localization signal; Zn, zinc finger DNA binding domain; PIISIQ, calcineurin-docking site; and SRR, serine-rich region) and the locations of potential Cdk phosphorylation sites (starred; S/TP). Phosphorylation of Crz1p was analyzed by SDS-PAGE and autoradiography. The positions of migration of phosphorylated Crz1p and Crz1(181–340)p are shown on the right.

(E) Activity of Crz1p in response to mutation of Pho85p and Hrr25p consensus sites. Cells carrying an integrated 4×CDRE::*lacZ* reporter (as in [B] above) bearing either vector (p415MET), a plasmid expressing wt *CRZ1* (Crz1: pAMS451), *CRZ1*T202A/S213A (Crz1TSA; pBA1793), *CRZ1*S231A/S234A (Crz1S2A; pBA1794), or a quadruple mutant of *CRZ1* (CRZ1T202A,S213A,S231A,S234A; pBA1795) from the inducible MET promoter were grown in selective medium lacking methionine to induce *CRZ1* expression. β-galactoside activity was measured as described in (B). Data are the mean (±SEM) of three independent isolates. No $CaCl_2$ was added to the cultures.

array. We failed to find an association between proteins with toxic overexpression phenotypes and proteins annotated as forming parts of complexes. Moreover, there was no general relationship between haploinsufficiency phenotypes and overexpression phenotypes, demonstrating that genes whose phenotypes are sensitive to decreased gene dosage are not especially likely to be sensitive to increased dosage. Thus, although the balance hypothesis may explain the dosage sensitivity for particular genes encoding subunits of complexes, it is unlikely to be a general explanation for haploinsufficiency phenotypes.

Our systematic survey reveals that most genes do not compromise cellular fitness when overexpressed, suggesting cellular mechanisms act to regulate or constrain the activity of proteins or regulatory pathways. Supporting this observation is the phenomenon of dosage compensation in *Drosophila melanogaster* and *Caenorhabitis elegans*, which involves regulating gene expression at the level of entire chromosomes. For example, in *D. melanogaster*, the level of transcription of the X chromosome in males (XY) relative to each X chromosome in females (XX) is increased by 2-fold (Straub et al., 2005). Although one additional copy of a gene appears unfavorable in flies and worms, our work suggests that yeast can cope with up to 50 copies (high-copy plasmid) of most genes (85%) expressed from a constitutive promoter.

We reasoned that regulatory networks compensating for gene overexpression may be revealed through systematic SDL screening, identifying overexpression phenotypes within the context of specific signaling mutant backgrounds. As proof of concept, we used the SGA method to introduce our overexpression array into a yeast strain lacking the Pho85 kinase. SGA allows introduction of marked alleles of a query gene into any appropriately marked yeast array through a series of replica pinning steps (Tong et al., 2004). In the case of our overexpression array, the simple pinning procedure effectively substitutes for many thousands of individual yeast transformations; because the plasmids are arrayed, genetic interactors can be immediately identified by their position on the array, enabling rapid and systematic overexpression genetics.

Our *pho85*Δ SDL screen identified several known targets of Pho85 as well as an additional substrate, Crz1p, which was also identified in a protein chip screen for kinase targets (Ptacek et al., 2005). The identification of Crz1p as a target for Pho80p-Pho85p reveals a physiological role for the Pho80p-Pho85p kinase, whose only previously appreciated substrate was the transcription factor Pho4, and establishes a link between a Cdk and calcium signaling. Both Pho80p-Pho85p and Crz1p/calcinerin mediate stress responses in yeast. These two conserved signaling pathways may activate Crz1p synergistically under environmental conditions, such as alkaline stress, that both trigger Ca^{2+} signaling and cause phosphate limitation (Serrano et al., 2002). Furthermore, the regulation of Crz1p by multiple kinases in budding yeast is analogous to the regulation of the mammalian functional homolog of Crz1p; nuclear export of NFAT responds to phosphorylation by multiple kinases, including casein kinase I, GSK3, PKA, and the MAP kinases p38 and JNK, depending on the NFAT isoform (Hogan et al., 2003). Our findings suggest a potential role for the Pho85p homolog Cdk5p in NFAT regulation. More generally, our results suggest that a combination of SDL and protein chip screens should prove a fruitful means for systematic analysis of kinase function. The combination of an overexpression array with the SGA genetic platform means that SDL screening is easily extensible to other genes.

The results presented here suggest that a major factor restricting inappropriate gene expression is the resulting detrimental phenotypes associated with hyperactive gain-of-function activity of overexpressed proteins. Moreover, gain-of-function phenotypes may only be manifested in specific contexts, such as particular disease situations. More generally, the exploitation of gain-of-function phenotypes within the context of genetically sensitized signaling mutants provides an approach for linking signaling molecules to substrates. Analogous screens combining gene overexpression with RNAi-mediated gene knockdown approaches should expand this strategy to higher eukaryotic cells and metazoan model systems.

Experimental Procedures

Yeast Array Construction

We amplified the p*GAL1/10*-driven GST-6×His plasmid library (Zhu et al., 2001; Zhu et al., 2000) in *E. coli*. Plasmid DNA was isolated by using a Qiagen Qiabot 8000 Biorobot. Miniprep DNA was introduced into strain Y4741 by using a high-throughput adaptation of a lithium acetate transformation method (Gietz and Woods, 2002). Two independent transformants were patched onto agar plates. Plates of 96 patches were converted into a 768 colony format by using a VersArray Colony Arrayer (BioRad). Each strain, possessing a unique high copy plasmid, is represented twice in the array. The entire array consists of 19 plates.

Systematic Examination of Genes Causing Slow Growth upon Overexpression

Using a VersArray Colony Arrayer (BioRad), the array was pinned to glucose or galactose containing medium. Digital photographs were taken after 2 or 3 days at 30ºC. The screen was repeated four times. Sensitivities were scored by an automated system that measures colony area from digital images and reports the probability (p value) that the area is different between glucose and galactose plates (C.B. and H. Ding, unpublished data). Eight (4 × 2) colonies from the glucose and galactose plates were compared. P values less than 0.1 were considered statistically significant. 994 strains were considered, by these criteria, to be significantly slow growing on galactose. Serial spot dilutions to glucose and galactose confirmed a slow-growth phenotype relative to a strain carrying an empty control plasmid (pEGH). Inability to grow was scored based on a number system: 1 (no growth) to 5 (wt growth). 769 strains were confirmed to be slow growing in the presence of galactose.

Morphological Profiling

For phenotypic profiling, strains were grown, fixed, stained, and examined by fluorescence microscopy. Briefly, strains were grown for 5 hr at 30ºC in synthetic media with 2% galactose, fixed by the addition of formaldehyde (3.7%), and stained with rhodamine-conjugated phalloidin (Molecular Probes), Fluorescence Brightener (Sigma), and 4′,6-diamidino-2-phenylindole (Sigma). At least 200 cells of each strain were examined by light and fluorescence microscopy. Strains were scored for the following morphological descriptors: an increase of unbudded, small-budded, or large-budded cells; small, large, or variable size; round, pointed, elongated, or amorphous shape; hyperpolarized buds; multiple buds; wide bud neck; lysed and clumped; multiple nuclei; diffuse chitin staining; bipolar budding; clustered mitochondria; aggregated actin patches; diffuse actin stain; and intense or absent actin cables. All phenotypes were

subclassified as slight, moderate, or severe. Cells were photographed with a CoolSNAP HQ high-speed digital camera (Roeper Scientific) mounted on a Leica DM-LB microscope. Images were captured and analyzed with MetaMorph software (Universal Imaging Media, PA).

FACS

The 184 strains identified as having a discernable morphological abnormality were grown, fixed, and subjected to FACS analysis. Briefly, strains were induced for 5 hr at 30ºC in synthetic media with 2% galactose, fixed in ethanol, and prepared for FACS analysis with Sytox Green (Molecular Probes). Samples were sonicated, and flow cytometry was carried out with a Becton Dickinson FACSCalibur and CellQuest Pro software (BD Biosciences). Events were modeled with ModfitLT 3.0 software (Verity Software House, Inc.). Percentage of DNA content was calculated by dividing the number of events under each DNA peak by the total number of events under all peaks.

Microarrays

Strains containing tagged *WHI3* and *WHI4* were grown in parallel with corresponding empty vector (pEGH) control cultures in selective media plus 2% raffinose to midlog phase, induced with 2% galactose for 3 hr, and frozen in liquid nitrogen. RNA preparation, hybridization, image acquisition, and processing of microarrays were performed as described (Grigull et al., 2004).

SDL Screening

A modification of the SGA method (Tong et al., 2001) was used to introduce the overexpression array into a strain deleted for *PHO85* (see Supplemental Experimental Procedures for details). A strain harboring *pho85*Δ was mated to the overexpression array by replica pinning. Diploids were selected and sporulated. *MAT*a *pho85 ΔpGALxxx* haploids were isolated through successive pinning steps on selective media and then pinned onto the same medium containing either 2% galactose or 2% glucose. Colonies on galactose plates were compared to glucose plates to identify those strains with a galactose-specific growth defect. Genes causing slow growth, upon overexpression, specifically in the absence of *PHO85* were identified by comparison to a roster of toxic genes. All SDL hits were confirmed by direct transformation followed by serial spot dilution assays.

Kinase Assays

Recombinant Pho80p-Pho85p kinase was expressed and purified from insect cells as described (Huang et al., 1999). Approximately 150 ng of exogenous substrate was added per reaction. Substrates included full-length Gst-Crz1p, and four truncated versions: amino acids 1–180, 181–340, 341–440, and 441–678 (all N-terminal Gst-fusion proteins). All fusions were expressed in *E. coli* and purified by using glutathione columns, followed by elution and dialysis into 20 mM HEPES (pH 6.8), 150 mM KOAc, 250 mM sorbitol, and 2 mM MgOAc. Kinase reactions were performed in 10 μL volumes containing 50 mM Tris-HCl at pH 7.5, 10 mM $MgCl_2$, 1 mM dithiothreitol, 1 μM cold ATP, and 1 μl $\gamma-3^2$P-ATP for 20 min at 30ºC. Reactions were stopped by addition of 2× sample buffer. Samples were resolved on 10% SDS-PAGE gels. Dried gels were exposed to autoradiographic film (Kodak Biomax; Kodak, Canada).

DNA Manipulations and Mutagenesis

All gene disruptions were achieved by homologous recombination at their chromosomal loci by standard polymerase-chain reaction (PCR)-based methods and verified by PCR and phenotypic analyses. Point mutants were made by PCR-based site-directed mutagenesis (see Supplemental Experimental Procedures for details).

Crz1p-GFP Localization

The localization of GFP-Crz1p was monitored upon calcium addition in a wt strain (BY263) and in the same strain overexpressing *PHO80* from a high-copy plasmid (pBA1810). One-hundred millimolars of $CaCl_2$ was added to the cultures in midlog phase, and time-lapse photography was used to visualize GFP-Crz1p after 2, 15, and 25 min. Cells were photographed with a Cascade 512B high-speed digital camera (Roeper Scientific) mounted on a Leica DM-LB microscope. Images were captured and analyzed by MetaMorph software (Universal Imaging Media, PA). See the Supplemental Experimental Procedures for numbers.

Quantitative β-Galactosidase Assays

CDRE-lacZ reporter assays were performed as described (Kafadar et al., 2003). Briefly, either (1) wt (BY263), *pho85*Δ (BY391), and *pho80*Δ (BY490) strains carrying plasmid pAMS366 or (2) strain ASY832 carrying empty vector or pBA1810 (p*GPD-PHO80*) was grown in selective media to midlog phase. For $CaCl_2$ induction tests, strains were diluted into media with the indicated concentrations of $CaCl_2$ and incubated 3 hr. Cells were harvested and broken open in lysis buffer (100 mM Tris-HCl [pH 8.0], 1 mM DTT, and 20% glycerol with protease inhibitors) with glass beads. The β-galactosidase activity was determined by adding 100 μl of total cell extracts to 0.9 ml of Z buffer (100 mM Na_2HPO_4, 40 mM NaH_2PO_4, 10 mM KCl, 1 mM $MgSO_4$, and 0.027% β-mercaptoethanol) and 200 μl ONPG (Sigma). Units of β-galactosidase activity were determined as described (Kafadar et al., 2003). The experiment shown in Figure 6E was done in the absence of calcium.

Supplemental Data

Supplemental Data include Supplemental Experimental Procedures, Supplemental References, one figure, and nine tables and can be found with this article online at http://www.molecule.org/cgi/content/full/21/3/319/DC1/.

Acknowledgments

We thank Waleed Anwar and Trinh Hoac for assistance with morphological database management and Huiming Ding for help with data analysis. As well, thanks to Dan Durocher for the use of his Beckman Becton Dickinson FACSCalibur. R.S. was supported by a Natural Sciences and Engineering Research Council of Canada (NSERC) postgraduate scholarship and a Terry Fox Foundation research studentship. G.C. was the recipient of a Best Foundation Fellowship. This work was supported by grants from the Canadian Institutes of Health Research to B.A. and C.B., Genome Canada through the Ontario Genomics Institute to B.A., C.B., and T.R.H., and the NSERC to C.B. and T.R.H. Equipment for our SGA screening laboratories was purchased with funds from the Canadian Foundation for Innovation and the Ontario Innovation Trust. Work in the Manchester laboratory was supported by grants to S.G.O. from the Biotechnology & Biological Sciences Research Council; B.P. was supported, in part, by a Human Frontiers Science Program Fellowship.

Received: October 8, 2005
Revised: November 24, 2005
Accepted: December 7, 2005
Published: February 2, 2006

References

Akada, R., Yamamoto, J., and Yamashita, I. (1997). Screening and identification of yeast sequences that cause growth inhibition when overexpressed. Mol. Gen. Genet. *254*, 267–274.

Boustany, L.M., and Cyert, M.S. (2002). Calcineurin-dependent regulation of Crz1p nuclear export requires Msn5p and a conserved calcineurin docking site. Genes Dev. *16*, 608–619.

Boyer, J., Badis, G., Fairhead, C., Talla, E., Hantraye, F., Fabre, E., Fischer, G., Hennequin, C., Koszul, R., Lafontaine, I., et al. (2004). Large-scale exploration of growth inhibition caused by overexpression of genomic fragments in Saccharomyces cerevisiae. Genome Biol. *5*, R72.

Cyert, M.S. (2003). Calcineurin signaling in *Saccharomyces cerevisiae*: how yeast go crazy in response to stress. Biochem. Biophys. Res. Commun. *311*, 1143–1150.

de Lichtenberg, U., Jensen, L.J., Fausboll, A., Jensen, T.S., Bork, P., and Brunak, S. (2005). Comparison of computational methods for the identification of cell cycle-regulated genes. Bioinformatics *21*, 1164–1171.

Deutschbauer, A.M., Jaramillo, D.F., Proctor, M., Kumm, J., Hillenmeyer, M.E., Davis, R.W., Nislow, C., and Giaever, G. (2005).

Mechanisms of haploinsufficiency revealed by genome-wide profiling in yeast. Genetics *169*, 1915–1925.

Espinet, C., de la Torre, M.A., Aldea, M., and Herrero, E. (1995). An efficient method to isolate yeast genes causing overexpression-mediated growth arrest. Yeast *11*, 25–32.

Forsburg, S.L. (2001). The art and design of genetic screens: yeast. Nat. Rev. Genet. *2*, 659–668.

Gari, E., Volpe, T., Wang, H., Gallego, C., Futcher, B., and Aldea, M. (2001). Whi3 binds the mRNA of the G1 cyclin CLN3 to modulate cell fate in budding yeast. Genes Dev. *15*, 2803–2808.

Gavin, A.C., Bosche, M., Krause, R., Grandi, P., Marzioch, M., Bauer, A., Schultz, J., Rick, J.M., Michon, A.M., Cruciat, C.M., et al. (2002). Functional organization of the yeast proteome by systematic analysis of protein complexes. Nature *415*, 141–147.

Giaever, G., Chu, A.M., Ni, L., Connelly, C., Riles, L., Veronneau, S., Dow, S., Lucau-Danila, A., Anderson, K., Andre, B., et al. (2002). Functional profiling of the Saccharomyces cerevisiae genome. Nature *418*, 387–391.

Gietz, R.D., and Woods, R.A. (2002). Transformation of yeast by lithium acetate/single-stranded carrier DNA/polyethylene glycol method. Methods Enzymol. *350*, 87–96.

Grigull, J., Mnaimneh, S., Pootoolal, J., Robinson, M., and Hughes, T.R. (2004). Genome-wide analysis of mRNA stability using transcription inhibitors and microarrays reveals posttranscriptional control of ribosome biogenesis factors. Mol. Cell. Biol. *24*, 5534–5547.

Henchoz, S., Chi, Y., Catarin, B., Herskowitz, I., Deshaies, R.J., and Peter, M. (1997). Phosphorylation- and ubiquitin-dependent degradation of the cyclin-dependent kinase inhibitor Far1p in budding yeast. Genes Dev. *11*, 3046–3060.

Herskowitz, I. (1987). Functional inactivation of genes by dominant negative mutations. Nature *329*, 219–222.

Ho, Y., Gruhler, A., Heilbut, A., Bader, G.D., Moore, L., Adams, S.L., Millar, A., Taylor, P., Bennett, K., Boutilier, K., et al. (2002). Systematic identification of protein complexes in Saccharomyces cerevisiae by mass spectrometry. Nature *415*, 180–183.

Hogan, P.G., Chen, L., Nardone, J., and Rao, A. (2003). Transcriptional regulation by calcium, calcineurin, and NFAT. Genes Dev. *17*, 2205–2232.

Huang, D., Patrick, G., Moffat, J., Tsai, L.H., and Andrews, B. (1999). Mammalian Cdk5 is a functional homologue of the budding yeast Pho85 cyclin-dependent protein kinase. Proc. Natl. Acad. Sci. USA *96*, 14445–14450.

Huang, D., Moffat, J., and Andrews, B. (2002). Dissection of a complex phenotype by functional genomics reveals roles for the yeast cyclin-dependent protein kinase Pho85 in stress adaptation and cell integrity. Mol. Cell. Biol. *22*, 5076–5088.

Hughes, T.R., Robinson, M.D., Mitsakakis, N., and Johnston, M. (2004). The promise of functional genomics: completing the encyclopedia of a cell. Curr Opin Microbiol *7*, 546–554.

Irniger, S., Piatti, S., Michaelis, C., and Nasmyth, K. (1995). Genes involved in sister chromatid separation are needed for B-type cyclin proteolysis in budding yeast. Cell *81*, 269–277.

Jorgensen, P., Nishikawa, J., Breitkreutz, B.-J., and Tyers, M. (2002). Systematic identification of pathways that couple cell growth and division in yeast. Science *297*, 395–400.

Kafadar, K.A., and Cyert, M.S. (2004). Integration of stress responses: modulation of calcineurin signaling in Saccharomyces cerevisiae by protein kinase A. Eukaryot. Cell *3*, 1147–1153.

Kafadar, K.A., Zhu, H., Snyder, M., and Cyert, M.S. (2003). Negative regulation of calcineurin signaling by Hrr25p, a yeast homolog of casein kinase I. Genes Dev. *17*, 2698–2708.

Kelley, R., and Ideker, T. (2005). Systematic interpretation of genetic interactions using protein networks. Nat. Biotechnol. *23*, 561–566.

Kim, H.B., Haarer, B.K., and Pringle, J.R. (1991). Cellular morphogenesis in the Saccharomyces cerevisiae cell cycle: localization of the CDC3 gene product and the timing of events at the budding site. J. Cell Biol. *112*, 535–544.

Krogan, N.J., Peng, W.T., Cagney, G., Robinson, M.D., Haw, R., Zhong, G., Guo, X., Zhang, X., Canadien, V., Richards, D.P., et al. (2004). High-definition macromolecular composition of yeast RNA-processing complexes. Mol. Cell *13*, 225–239.

Kroll, E.S., Hyland, K.M., Hieter, P., and Li, J.J. (1996). Establishing genetic interactions by a synthetic dosage lethality phenotype. Genetics *143*, 95–102.

Liu, H., Krizek, J., and Bretscher, A. (1992). Construction of a GAL1-regulated yeast cDNA expression library and its application to the identification of genes whose overexpression causes lethality in yeast. Genetics *132*, 665–673.

Manning, G., Plowman, G.D., Hunter, T., and Sudarsanam, S. (2002). Evolution of protein kinase signaling from yeast to man. Trends Biochem. Sci. *27*, 514–520.

Measday, V., and Hieter, P. (2002). Synthetic dosage lethality. Methods Enzymol. *350*, 316–326.

Measday, V., Hailey, D.W., Pot, I., Givan, S.A., Hyland, K.M., Cagney, G., Fields, S., Davis, T.N., and Hieter, P. (2002). Ctf3p, the Mis6 budding yeast homolog, interacts with Mcm22p and Mcm16p at the yeast outer kinetochore. Genes Dev. *16*, 101–113.

Measday, V., Baetz, K., Guzzo, J., Yuen, K., Kwok, T., Sheikh, B., Ding, H., Ueta, R., Hoac, T., Cheng, B., et al. (2005). Systematic yeast synthetic lethal and synthetic dosage lethal screens identify genes required for chromosome segregation. Proc. Natl. Acad. Sci. USA *102*, 13956–13961.

Mewes, H.W., Amid, C., Arnold, R., Frishman, D., Guldener, U., Mannhaupt, G., Munsterkotter, M., Pagel, P., Strack, N., Stumpflen, V., et al. (2004). MIPS: analysis and annotation of proteins from whole genomes. Nucleic Acids Res. *32*, D41–D44.

Mnaimneh, S., Davierwala, A.P., Haynes, J., Moffat, J., Peng, W.T., Zhang, W., Yang, X., Pootoolal, J., Chua, G., Lopez, A., et al. (2004). Exploration of essential gene functions via titratable promoter alleles. Cell *118*, 31–44.

Moffat, J., and Andrews, B. (2004). Late-G1 cyclin-CDK activity is essential for control of cell morphogenesis in budding yeast. Nat. Cell Biol. *6*, 59–66.

Moffat, J., Huang, D., and Andrews, B.J. (2000). Functions of Pho85 cyclin-dependent kinases in budding yeast. Prog. Cell Cycle Res. *4*, 97–106.

Nash, R.S., Volpe, T., and Futcher, B. (2001). Isolation and characterization of WHI3, a size-control gene of Saccharomyces cerevisiae. Genetics *157*, 1469–1480.

Pan, X., Yuan, D.S., Xiang, D., Wang, X., Sookhai-Mahadeo, S., Bader, J.S., Hieter, P., Spencer, F., and Boeke, J.D. (2004). A robust toolkit for functional profiling of the yeast genome. Mol. Cell *16*, 487–496.

Papp, B., Pal, C., and Hurst, L.D. (2003). Dosage sensitivity and the evolution of gene families in yeast. Nature *424*, 194–197.

Polizotto, R.S., and Cyert, M.S. (2001). Calcineurin-dependent nuclear import of the transcription factor Crz1p requires Nmd5p. J. Cell Biol. *154*, 951–960.

Ptacek, J., Devgan, G., Michaud, G., Zhu, H., Zhu, X., Fasolo, J., Guo, H., Jona, G., Breitkreutz, A., Sopko, R., et al. (2005). Global analysis of protein phosphorylation in yeast. Nature *438*, 679–684.

Rorth, P., Szabo, K., Bailey, A., Laverty, T., Rehm, J., Rubin, G.M., Weigmann, K., Milan, M., Benes, V., Ansorge, W., and Cohen, S.M. (1998). Systematic gain-of-function genetics in *Drosophila*. Development *125*, 1049–1057.

Saito, T.L., Ohtani, M., Sawai, H., Sano, F., Saka, A., Watanabe, D., Yukawa, M., Ohya, Y., and Morishita, S. (2004). SCMD: Saccharomyces cerevisiae morphological database. Nucleic Acids Res. *32*, D319–D322.

Scherens, B., and Goffeau, A. (2004). The uses of genome-wide yeast mutant collections. Genome Biol. *5*, 229.

Serrano, R., Ruiz, A., Bernal, D., Chambers, J.R., and Arino, J. (2002). The transcriptional response to alkaline pH in Saccharomyces cerevisiae: evidence for calcium-mediated signaling. Mol. Microbiol. *46*, 1319–1333.

Stathopoulos, A.M., and Cyert, M.S. (1997). Calcineurin acts through the CRZ1/TCN1-encoded transcription factor to regulate gene expression in yeast. Genes Dev. *11*, 3432–3444.

Stathopoulos-Gerontides, A., Guo, J.J., and Cyert, M.S. (1999). Yeast calcineurin regulates nuclear localization of the Crz1p transcription factor through dephosphorylation. Genes Dev. *13*, 798–803.

Stevenson, L.F., Kennedy, B.K., and Harlow, E. (2001). A large-scale overexpression screen in Saccharomyces cerevisiae identifies previously uncharacterized cell cycle genes. Proc. Natl. Acad. Sci. USA *98*, 3946–3951.

Straub, T., Dahlsveen, I.K., and Becker, P.B. (2005). Dosage compensation in flies: mechanism, models, mystery. FEBS Lett. *579*, 3258–3263.

Tong, A.H., Evangelista, M., Parsons, A.B., Xu, H., Bader, G.D., Page, N., Robinson, M., Raghibizadeh, S., Hogue, C.W., Bussey, H., et al. (2001). Systematic genetic analysis with ordered arrays of yeast deletion mutants. Science *294*, 2364–2368.

Tong, A.H., Lesage, G., Bader, G.D., Ding, H., Xu, H., Xin, X., Young, J., Berriz, G.F., Brost, R.L., Chang, M., et al. (2004). Global mapping of the yeast genetic interaction network. Science *303*, 808–813.

Veitia, R.A. (2002). Exploring the etiology of haploinsufficiency. Bioessays *24*, 175–184.

Veitia, R.A. (2005). Gene dosage balance: deletions, duplications and dominance. Trends Genet. *21*, 33–35.

Wagner, A. (2005). Energy constraints on the evolution of gene expression. Mol. Biol. Evol. *22*, 1365–1374.

Wang, H., Gari, E., Verges, E., Gallego, C., and Aldea, M. (2004). Recruitment of Cdc28 by Whi3 restricts nuclear accumulation of the G1 cyclin-Cdk complex to late G1. EMBO J. *23*, 180–190.

Whiteway, M., Hougan, L., and Thomas, D.Y. (1990). Overexpression of the STE4 gene leads to mating response in haploid Saccharomyces cerevisiae. Mol. Cell. Biol. *10*, 217–222.

Winzeler, E.A., Shoemaker, D.D., Astromoff, A., Liang, H., Anderson, K., Andre, B., Bangham, R., Benito, R., Boeke, J.D., Bussey, H., et al. (1999). Functional characterization of the S. cerevisiae genome by gene deletion and parallel analysis. Science *285*, 901–906.

Zhang, L.V., King, O.D., Wong, S.L., Goldberg, D.S., Tong, A.H.Y., Lesage, G., Andrews, B., Bussey, H., Boone, C., and Roth, F.P. (2005). Motifs, themes and thematic maps of an integrated Saccharomyces cerevisiae interaction network. J. Biol. *4*, 6.1–6.31.

Zhang, N., Gardner, D.C., Oliver, S.G., and Stateva, L.I. (1999). Down-regulation of the expression of PKC1 and SRB1/PSA1/VIG9, two genes involved in cell wall integrity in *Saccharomyces cerevisiae*, causes flocculation. Microbiol. *145*, 309–316.

Zhu, H., Klemic, J.F., Chang, S., Bertone, P., Casamayor, A., Klemic, K.G., Smith, D., Gerstein, M., Reed, M.A., and Snyder, M. (2000). Analysis of yeast protein kinases using protein chips. Nat. Genet. *26*, 283–289.

Zhu, H., Bilgin, M., Bangham, R., Hall, D., Casamayor, A., Bertone, P., Lan, N., Jansen, R., Bidlingmaier, S., Houfek, T., et al. (2001). Global analysis of protein activities using proteome chips. Science *293*, 2101–2105.